

Research Article

Optimization on Operation Parameters in Reinforced Metal Matrix of AA6066 Composite with HSS and Cu

Y. Sesharao,¹ T. Sathish ,² Kumaran Palani ,³ Anjibabu Merneedi,⁴ Natrayan L ,² Melvin Victor De Poures ,² and T. Maridurai²

¹Department of Mechanical Engineering, QIS College of Engineering and Technology, Ongole 523272, Andhra Pradesh, India

²Department of Mechanical Engineering, Saveetha School of Engineering, SIMATS, Chennai 600 125, Tamil Nadu, India

³Department of Mechanical Engineering, Wolaita Sodo University, Wolaita Sodo Post Box- 138, Ethiopia

⁴Department of Mechanical Engineering, Aditya College of Engineering, Surampalem 533437, Andhra Pradesh, India

Correspondence should be addressed to Kumaran Palani; pkumaran2003et@gmail.com

Received 30 May 2021; Revised 16 June 2021; Accepted 22 June 2021; Published 2 July 2021

Academic Editor: Samson Jerold Samuel Chelladurai

Copyright © 2021 Y. Sesharao et al. This is an open access article distributed under the Creative Commons Attribution License, which permits unrestricted use, distribution, and reproduction in any medium, provided the original work is properly cited.

This optimization investigation focused on the reinforced metal matrix composite of aluminium alloy. Novel of this work is to fabricate the AA6066 composite with HSS and Cu, continually conduct machining tests, and evaluate the tool wear, surface roughness, and thrust force of the stir-casted specimens. The aluminium composite has 90 percentage of AA6066 alloy reinforcement with six percentage of high-speed steel and four percentage of copper alloy made by the casting method. The fabricated composites' turning parameters were optimized through the Taguchi method. The turning operation can be done with the help of the normal lathe with the CBN insert tool. The operation parameters such as feed, depth of cut, and steam pressure of the cutting fluid were considered with three different equal intervals in each parameter. In this investigation, the L9 orthogonal array method is used to identify the optimum values of the turning parameters among the considered machining parameters concerning the response such as wear on the turning tool and thrust forces created on machining. The outcome based on the parameters was identified and mentioned as the rank order for individual and combination of all responses with different conditions. Then, the separate and combined optimized input parameters were provided as the conclusion.

1. Introduction

Every operation needed various input parameters with respect to the different operating conditions. These parameters maybe less or more; it depends on the process and output. Among the various parameters, specifically, some of them create more impact on the desirable output on the machining. These parameters' optimization helps to enhance the machining or processing of the materials. So, the optimization of the various inputs of an experiment is needed to identify the most appropriate and preferable output in the accessible available resources. Sathish et al. [1] experimentally explained about the optimization on the machining constraints of the zirconium carbide (ZrC) reinforced aluminium alloy of AA7155 aluminium alloy composites.

Sabarirajan et al. [2] obviously discussed about the AA6063 aluminium alloy reinforcement with the silicon carbide machining parameter optimization by using the Taguchi method with different specific diagrams related to the experimental outcomes. Sevel et al. [3] gave details regarding optimizing of the parameters of the method of laser welding on the butt joints of the AA7068 aluminium alloys with clear diagrammatic representations of the main effect plots with priority order of the considered parameters. Sathish [4] individually investigated the parameters of the electro chemical process by the Taguchi method and explained the clear method of the optimization technique with respect to the reactions of experimental results.

Dinesh Kumar et al. [5] completely explained about the progression parameters of A-GTAW welding process based on the contribution parameters of the joining process by

means of the help of the different plots of the foremost effects. Saravanan et al. [6] entirely explained about the optimization method for the solar flat plate collector with nanofluids of aluminium nitride-based temperature differences through the help of the Minitab software by using the Taguchi method. Muthukumar et al. [7] entirely discussed the step-by-step procedure for the optimization methods with various contour plots by different colour representations on the various ranges of experimental results.

Palaniappan et al. [8] effusively discussed about the turning process parameter-based optimization methods with three different responses to identify the optimum input parameters. They also explained with different plots and tables for the clear vision to identify the parameters. Rajesh et al. [9] completely focused the surface roughness in machining participation for the metal matrix composites of aluminium alloy of AA5083 composite created with the combination of the boron carbide materials. Gurusami et al. [10] obviously explained roughly the optimization in the stir casting process inputs for the rate of corrosion encouragement on the composite materials of the boron carbide reinforcement of the aluminium alloy AA7068.

In the same way, Shetty et al. [11] absolutely discussed about the metal matrix composite-related optimization of the nearly five inputs for the nearly five outputs in turning operation by using the specified tool. The standard lathe machine is practiced at this juncture for the investigation. They also considered the cutting fluid parameters such as steam pressure and diameter of the nozzle. Correspondingly, various forces involved were considered in the turning operation. Natrayan et al. [12] investigated Al-SiC and Al-Al₂O₃ with the help of the powder metallurgy technique. The author completely explained about the various characteristics, compositions of chemicals, and processing methods of the Al-SiC and Al-Al₂O₃ composites.

Georgantzia et al. [13] entirely explained about the various applications of the AA6XXX series in structural elements with various sizes and different shapes, welding process on different places, and bolted equipment design application, and more than that, they were clearly mentioned with the help of various research articles. Davim [14] clearly explained about the turning process cutting parameter-based optimization with the orthogonal arrays in the machining by the normal lathe machine. The considered input parameters were feed, speed, depth of cut, input range, force on the tool, thrust force applied, input voltage, and motor specifications.

Ramnath et al. [15] absolutely reviewed by means of various research articles and explained about the aluminium matrix composites. They explained the various basic experiments and parameter-based optimization of aluminium matrix composites individually reinforced with silicon carbide, aluminium oxide, boron carbide, fiber, zircon, and fly ash. They also summarized the individual special qualities of the abovementioned combination reinforced composites. Shukla et al. [16] identified the separate individual activities of reinforcement composites of silicon carbide used in aluminium which were studied with respect to the consequences of the mechanical properties of the composites such as microstructure effect, toughness, hardness, and tensile

strength. They also explained the various casting techniques used to produce the metal matrix composites.

Verma et al. [17] explained about the influence of difference of silicon and copper contents in aluminium composite alloy produced by the stir casting method. They castoff the copper content from 0.015% to 5.97% and silicon carbide content from 2.02% to 8.6% in the remaining aluminium alloy for the casting process. They correspondingly mentioned that the greatest mechanical properties were formed with increased copper content in the composites. Singla et al. [18] successfully explained about the improvement aluminium reinforcement with silicon carbide-based metal matrix for the optimization process based on the experimental results of the hardness; the maximum percentage of the silicon involvement proved the enhancement on the hardness on the composite material microstructures. Standard high-pressure hydrogen storage vessel, hydraulic valves, high-stressed components used in the machineries, air wings' part, and mobile industry apparatus were fabricated by AA6066 alloy.

Alaneme and Aluko [19] effectively discussed about the fabrication besides age-hardening actions of the composite of aluminium with the silicon carbide for the creation of the aluminium magnesium and silicon composite through the technique of stir casting. Pawar et al. [20] efficiently conversed regarding the aluminium-reinforced composite of the silicon carbide with the application on the spur gear. They also provided various applications of the same composite materials. Natrayan et al. [21] entirely studied about the mechanical property-based input impact of the aluminium composite materials. They only focused the tensile strength of the composite material which concludes that the increase of the silicon carbide is directly proportional to the increase in the tensile strength of the composites. Merneedi et al. applied the ICCM method to investigate the variation of nondimensional natural frequencies of an elliptical and rectangular thin plate by changing the position, size, and number of cut outs in all the possible ways to investigate their effects on the natural frequency of the plate; the same method can also be implemented for the analysis of composite plates [22].

In this work, based on the optimization of the machining parameter such as feed rate, depth of cut with the cutting fluid pressure for the reinforced composite of AA6066 aluminium alloy with high-speed steel and copper is created by way of casting. These contribution considerations of the machining optimization are based on the experimental consequences of the tool wear in addition to the thrust force created at the time of machining with the help of the Taguchi method L9 orthogonal array. These two consequences were optimized separately and in a together manner.

2. Experimental Setup

This experimental investigation is mainly focused on the turning parameters of the reinforced metal matrix composites. Initially, the metal-reinforced specimens were prepared by the casting method [23]. The composition of the AA6066 aluminium alloy is mentioned in Table 1, and the remaining percentage is occupied by the pure aluminium

TABLE 1: Chemical opus of aluminium alloy (AA6066).

Composition	Silicon (%)	Magnesium (%)	Copper (%)	Manganese (%)	Chromium (%)
Percentage	1.80	1.40	1.20	1.10	0.40

alloy. The main contribution as 90 percentage of AA6066 alloy is reinforced with 6% of high-speed steel and 4% of copper alloy in the total percentage of the volume of the weight in the composite formation. All the materials were collected in the powder form from the online purchase. Then, the mixed materials were poured into the combustion chambers with 50,000 C and 500 kW capacity for one hour beyond the molten metal temperature.

Then, the molten metal has the mixture of all powder materials which are poured into the mould cavities for casting. The mould cavities were created as per the requirement of the specimen sizes. As per Figure 1(a), 30 mm diameter and 120 mm length cylindrical specimens were created from the casting method. Then, casted specimens were cleaned and inspected visually, such as size, cracks, and damage, for the second stage of the experiments. The normal traditional lathe machine is chosen for this investigation mentioned in Figure 1(b). It has the following specification: 5 kW motor, screw-guided automatic feed from 0.05 to 2 mm, and tool post and tail stock can be easily movable. Three Jaw chuck job holder is used in this experiment. The tool involved here is the inserts of cubic boron nitride (CBN). In this machining, the cutting fluid is steam with adjustable pressure from 1 bar to 15 bar with the nozzle arrangement in the end of the fluid flow [24].

There are 20 specimens that were created for the experiment, but nine clear defectless specimens are enough to conduct these experiments. Before conducting the experiment, the environment of the machine should be clean, and the cutting fluid should be ready to produce the steam using the electric heater. The CBN tool is fixed in the tool post as per the turning operation. The prepared specimen is fixed in the three-jaw chuck which is tightly fixed by the tools. The center of the specimen is checked properly. The turning distance as per Figure 1(b) is measured by the vernier scale and marked by the black marker. The motor is worked in the counterclockwise direction for this operation. The feed and depth of cut can be fixed by the rotating screw arrangement, and also, the pressure of the cutting fluid is controlled by the controller and monitored by the pressure gauge.

There are three inputs that were taken for the consideration of optimization with respect to the three desired outputs. The considered inputs were pressure of the cutting fluid (P_r), feed in mm per revolution (F), and cutting depth in millimetre (D) as per Table 2. These values were measured with the help of one pressure sensor on the feed tube, one contact sensor on the feed rotating threaded shaft, and a noncontact sensor in the machining place; these all are individually connected to the machine.

The desired outputs were rate of wear on the tool (TW), roughness on the surface (SR) of the machined specimens, and applied force of thrust (TF). Similarly, these all are also measured with the help of the sensors and dynamometer of

the lathe tool. There are 9 combinations, as per Table 2, that were created one by one with respect to the input parameters, and the corresponding values of the outputs were also measured for the clear identification. Each specimen is named as per Table 1 such as SN 1 to SN 9. The initial specimens before machining have the diameter of 30 mm and length of 120 mm, which are turned up to 80 mm length with diameter of 14 mm as per Figure 1(a). All the specimens have been machined in the same dimensions to recognize comparison on the results from each specimen for the considered conditions.

3. Results and Discussion

The wear on the tool on the end of the machining, machined surface roughness, and applied thrust forces of the individual specimens such as SN 1, SN 2, SN 3, SN 4, SN 5, SN 6, SN 7, SN 8, and SN 9 are measured and tabulated in Table 3 in a clear manner. L9 orthogonal array used the Taguchi method here to identify the maximum suitable inputs for the machining. All these three outputs come under the category of smaller is better condition. Because of the user expecting the minimum wear, minimum roughness and lowest thrust force were applied. The individual outputs and combinations of all the output were considered. Taguchi method results by using the Minitab 18 were discussed one by one in the sequence order.

3.1. Tool Wear. Initially, wear on the tool while performing the turning process on the concerned reinforced metal matrix of the aluminium alloy response ranks is tabulated in Table 4 under the condition that the minimum is the suitable.

The corresponding important effect diagram in Figure 2 expresses that the minimum wear rate was reached at 3 bar pressure of the cutting fluid with 0.15 mm per revolution of feed and 0.6 mm of cutting depth; similarly, the maximum wear rate can be obtained on 9 bar of cutting fluid pressure with the 0.10 mm per revolution of feed and 0.9 mm of cutting depth. This is also confirmed by the important effect diagram for the means of the wear rate measured in all the specimens in Figure 3.

There are four diagram representations that are available in a single diagram in Figure 4. It explained the percent with residuals which all are nearly closer to the normal probability line. This gives the reliability of the experiment results. Fitted values with residual relations clearly mentioned the diversion of the point of the results. There is a linear shape only formed in the frequency and residual comparison. Also, there are more than half number of crosses that were available in the versus order plot; it supports the experiment results of wear.

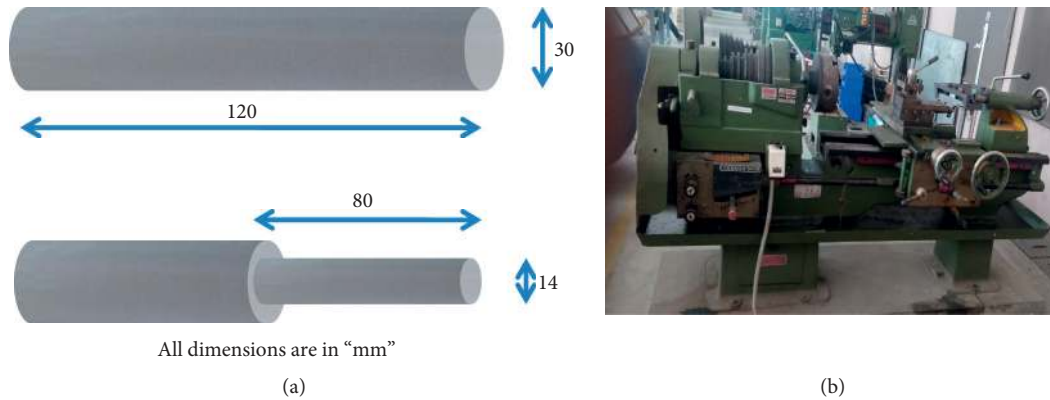


FIGURE 1: (a) Machining dimensions of the specimens. (b) Lathe machine used for this investigation.

TABLE 2: Input parameters variation as per the L9 method.

Specimen's number	Pressure of cutting fluid, P_r (bar)	Feed, F (mm/rev)	Depth of cut, D (mm)
SN 1	3	0.1	0.3
SN 2	3	0.15	0.6
SN 3	3	0.2	0.9
SN 4	6	0.1	0.6
SN 5	6	0.15	0.9
SN 6	6	0.2	0.3
SN 7	9	0.1	0.9
SN 8	9	0.15	0.3
SN 9	9	0.2	0.6

TABLE 3: Stir casting process parameters and its levels.

Specimen's number	TW (mm)	SR (μm)	TF (N)
SN 1	1.003	3.89	50.335
SN 2	0.493	2.85	15.385
SN 3	1.543	4.95	59.998
SN 4	0.893	2.27	17.51
SN 5	1.545	3.61	52.483
SN 6	0.653	2.45	21.15
SN 7	1.445	4.77	71.814
SN 8	0.823	2.39	40.563
SN 9	1.248	4.66	85.407

TABLE 4: Tool wear response ratios of signal to noise.

Level	Pressure of cutting fluid, P_r (bar)	Feed, F (mm/rev)	Depth of cut, D (mm)
1	0.7832	-0.7468	1.7892
2	0.3020	1.3522	1.7339
3	-1.1432	-0.6633	-3.5811
Delta	1.9265	2.0990	5.3703
Rank	3	2	1

3.2. *Surface Roughness.* Table 5 provides the surface roughness response for ratios of signal to noise with the ranks. Figure 5 provides the important effect diagram based on the roughness on the machined surface. The least amount surface roughness on the machined surface was obtained at the cutting fluid pressure of 6 bar with 0.15 mm per

revolution of feed and 0.3 mm of cutting depth; similarly, highest roughness on the machined surface can be obtained on 9 bar of cutting fluid pressure with 0.20 mm per revolution of feed and 0.9 mm of cutting depth. All these values were confirmed with the help of the mean-based important diagram in Figure 6 for roughness on the machined surface.

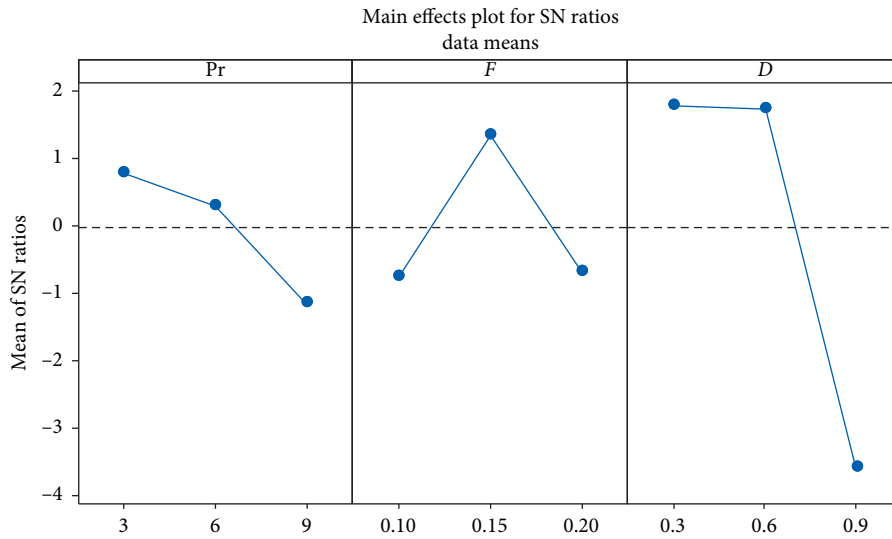


FIGURE 2: SN ratio-based important effect plot for wear on the tool; in the X-axis, Pr denotes pressure of cutting fluid (bar), F denotes feed (mm/rev), and D denotes depth of cut (mm).

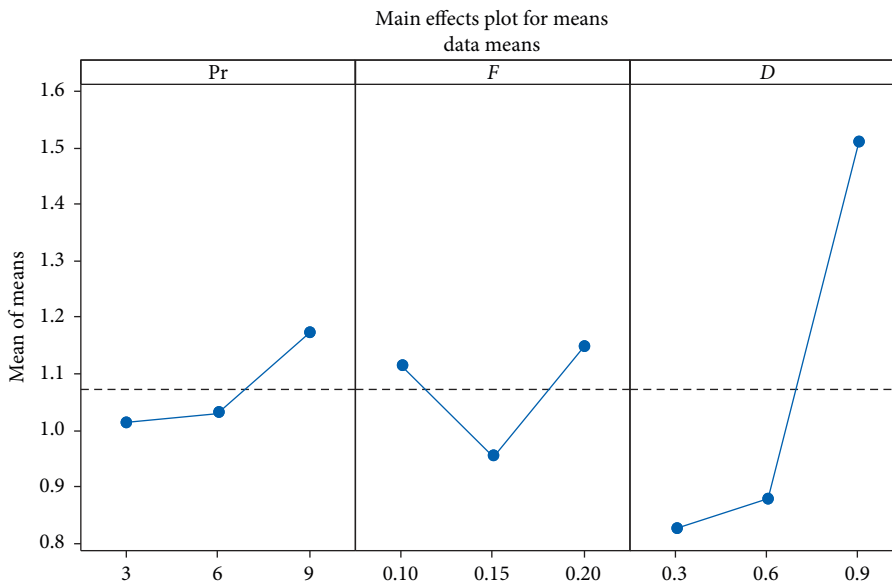


FIGURE 3: Mean-based important effect diagram for wear on the tool; in the X-axis, Pr denotes pressure of cutting fluid (bar), F denotes feed (mm/rev), and D denotes depth of cut (mm).

Figure 7 gives explanation about the four variation plots in the single diagram. It contains the points almost closer to the normal probability line in percent with residuals' variations. This provides the experiment outcomes reliability. Then, the fitted values with residual relations are mentioned. In the frequency and residual comparison, a linear shape is created. Also, there are less than half number of crosses that were obtained in the versus order plot.

3.3. *Thrust Force.* Table 6 mentions the thrust force-based response for ratios of signal to noise with the ranks. Figure 8 provides the important effect diagram based on the thrust force. The lowest amount thrust force is enough at the cutting fluid pressure of 6 bar with 0.15 mm per revolution of feed and 0.6 mm of cutting depth; similarly, greatest thrust force is needed at 9 bar of cutting fluid pressure with 0.20 mm per revolution of feed and 0.9 mm of cutting depth.

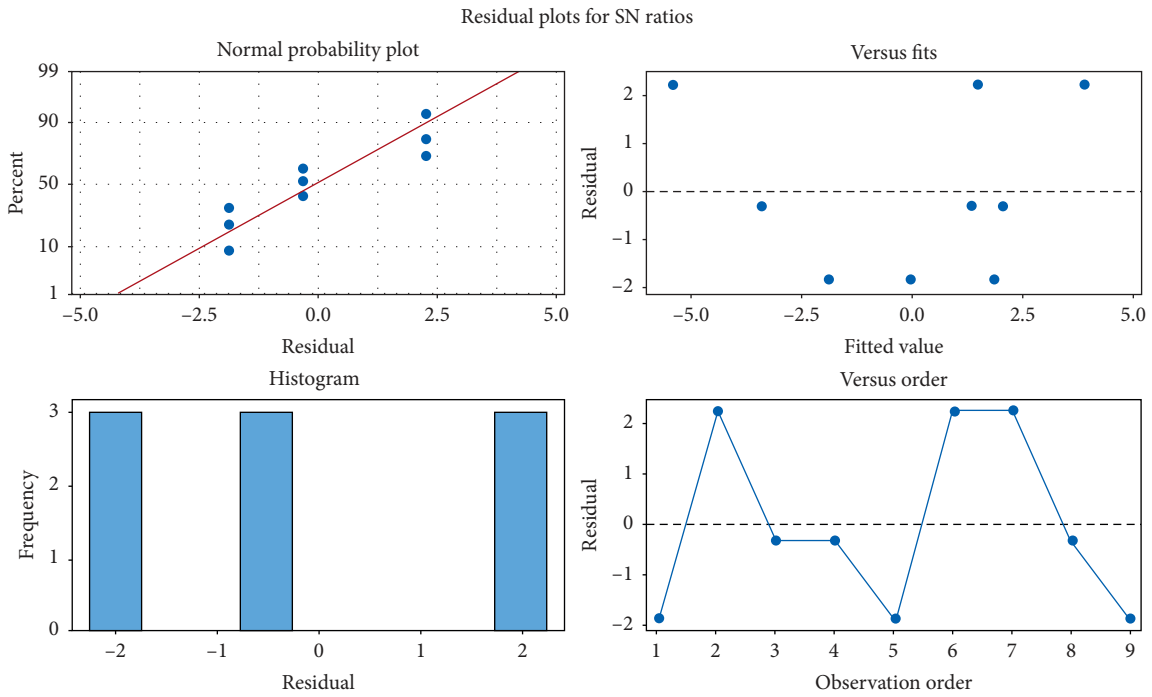


FIGURE 4: Tool wear’s residual plot of percent, frequency, fitted values, and observation order.

TABLE 5: Surface roughness on the machined surface response ratios of signal to noise.

Level	Pressure of cutting fluid, P_r (bar)	Feed, F (mm/rev)	Depth of cut, D (mm)
1	-11.596	-10.830	-9.050
2	-8.685	-9.272	-9.862
3	-11.502	-11.681	-12.871
Delta	2.911	2.409	3.821
Rank	2	3	1

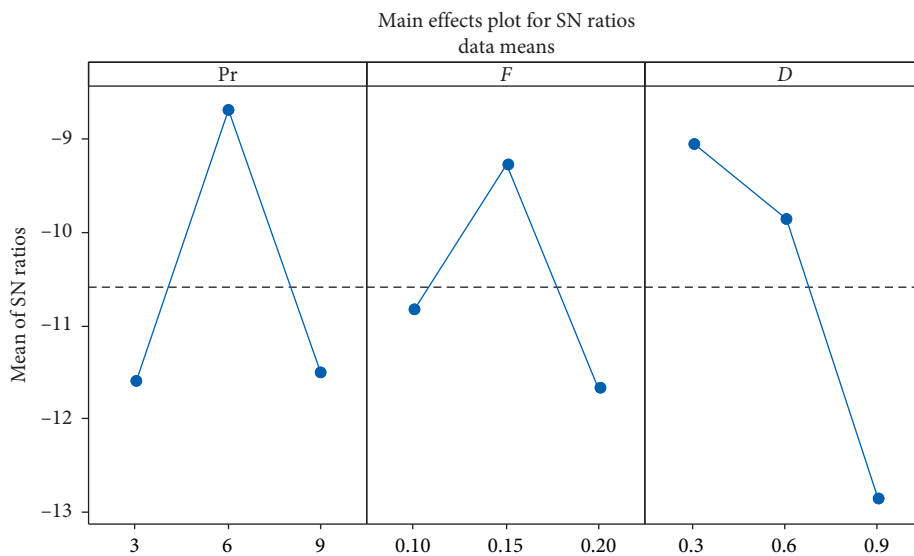


FIGURE 5: SN ratio-based important effect plot for the roughness on the machined surface; in the X-axis, P_r denotes pressure of cutting fluid (bar), F denotes feed (mm/rev), and D denotes depth of cut (mm).

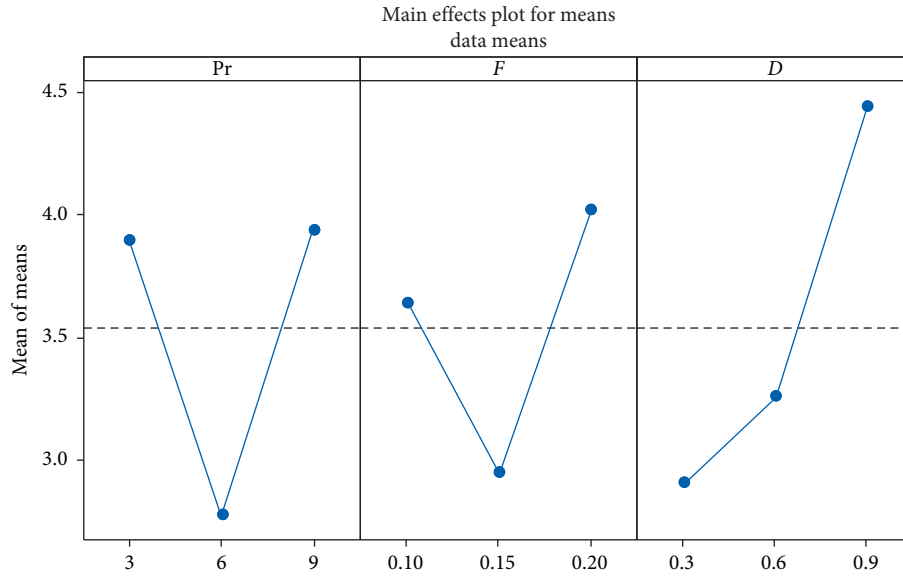


FIGURE 6: Mean-based important effect diagram for the roughness on the machined surface; in the X-axis, Pr denotes pressure (bar), F denotes feed (mm/rev), and D denotes depth of cut (mm).

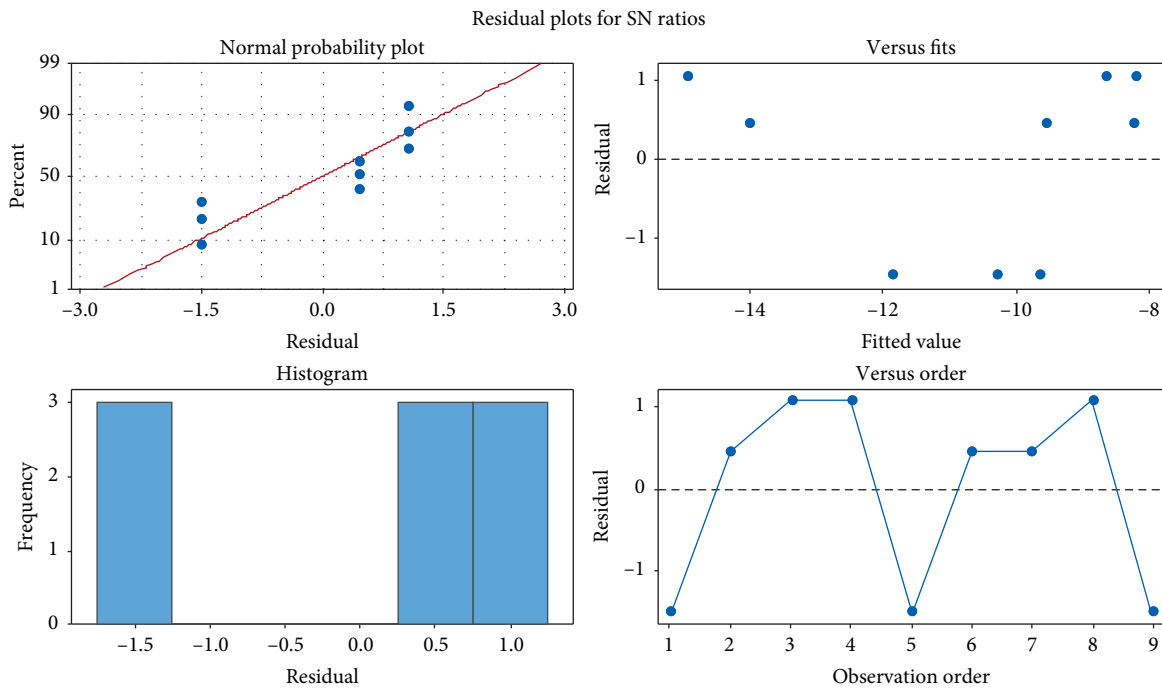


FIGURE 7: Surface roughness on machined surface residual plot of percent, frequency, fitted values, and versus order.

Figure 9 also corroborates the same results' confirmation based on the mean values of the thrust force applied on the specimens during the process of machining. Figure 10 mentions the explanation about various four plots in one diagram. These residuals-based percent and fitted values' plot gives the reliabilities of the experimental results. Then, the frequencies give the linear shape with gaps in the residuals.

Then, versus order gives more than half experiment results crossing the mean line. So, the results have the good quality.

3.4. *Combination of Response.* The three-response-based important diagram is clearly shown in Figure 11. The smaller amount of all these responses was reached at the parameters

TABLE 6: Thrust force-based response ratios of signal to noise.

Level	Pressure of cutting fluid, P_r (bar)	Feed, F (mm/rev)	Depth of cut, D (mm)
1	-31.11	-32.01	-30.90
2	-28.59	-30.10	-29.08
3	-35.97	-33.57	-35.70
Delta	7.38	3.46	6.62
Rank	1	3	2

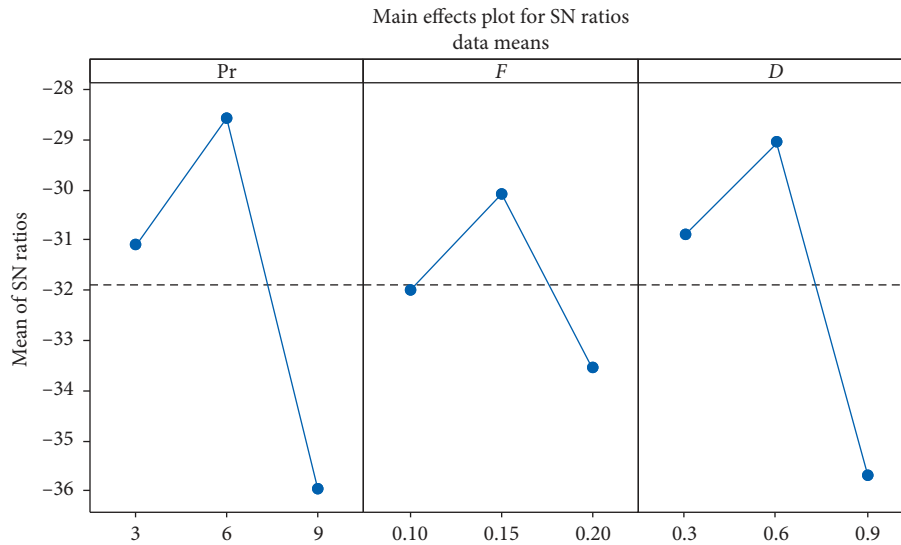


FIGURE 8: Thrust force-based important diagram based on the ratio of SN; in the X-axis, P_r denotes pressure of cutting fluid (bar), F denotes feed (mm/rev), and D denotes depth of cut (mm).

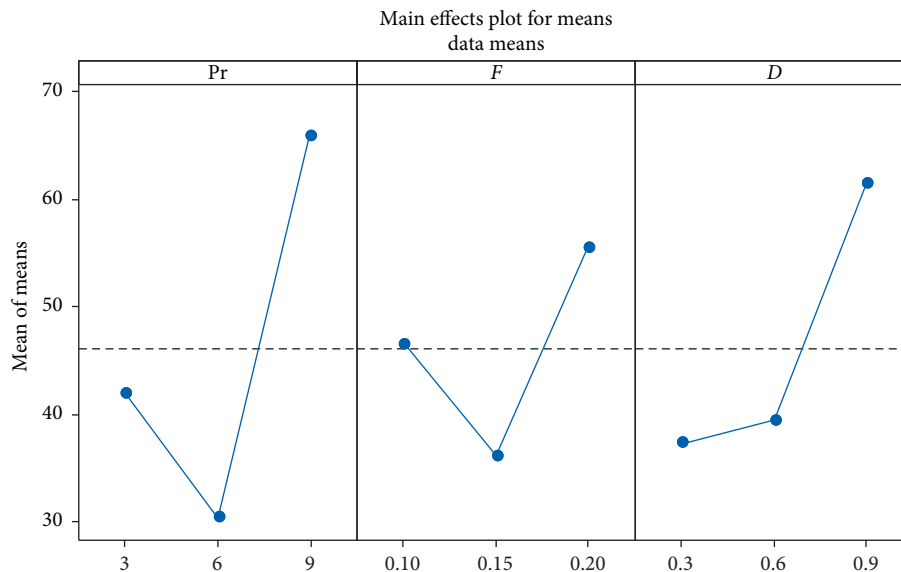


FIGURE 9: Thrust force-based important diagram based on the means; in the X-axis, P_r denotes pressure of cutting fluid (bar), F denotes feed (mm/rev), and D denotes depth of cut (mm).

for the cutting fluid pressure of 6 bar with 0.15 mm per revolution of feed and 0.6 mm of cutting depth; in the same way, highest thrust force was reached at 9 bar of cutting fluid pressure with 0.20 mm per revolution of feed and 0.9 mm of cutting depth; these all are confirmed by Figure 12 based on

the mean values of the process parameters. Tool wear, surface roughness, and thrust force-based signal-to-noise response are mentioned in Table 7 with the ranks.

Residual diagrams based on SN ratios for tool wear, surface roughness, and thrust force-related plot are shown in

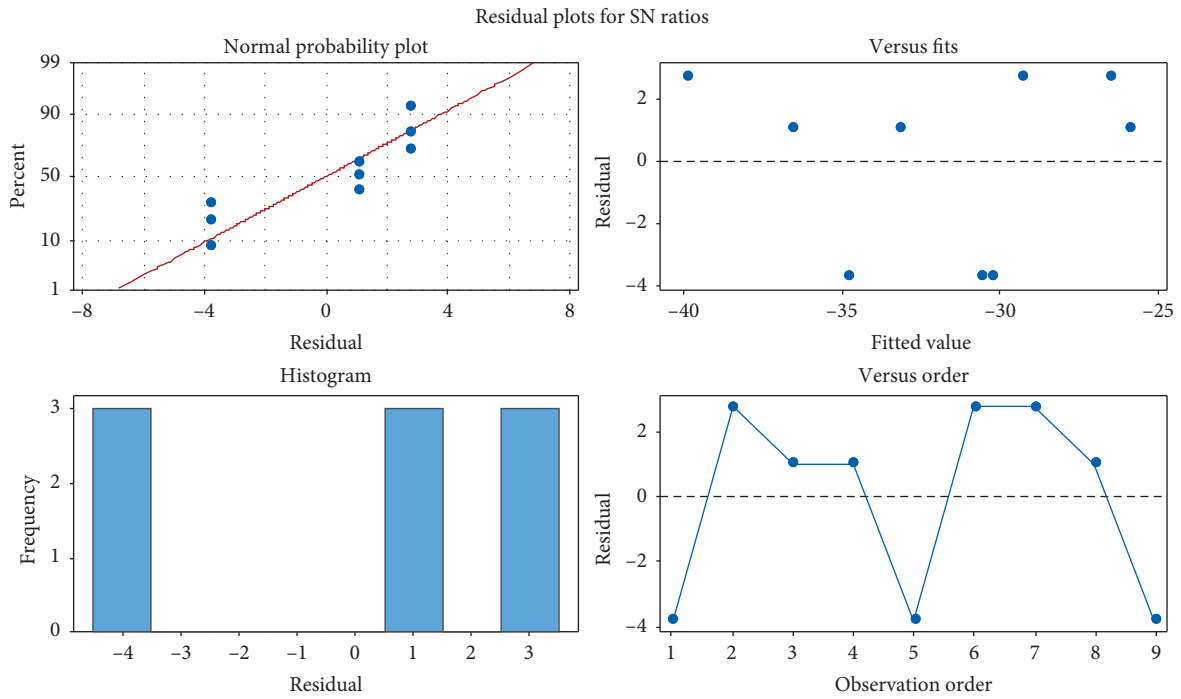


FIGURE 10: Thrust force-based residual plot of percent, frequency, fitted values, and versus order.

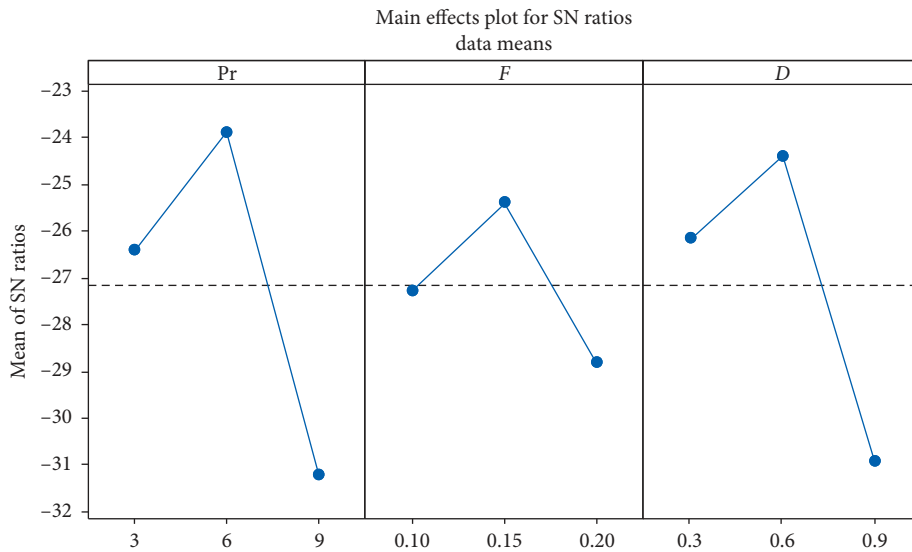


FIGURE 11: Tool wear, surface roughness, and thrust force focused the important diagram-based on the ratio of SN; in the X-axis, pressure of cutting fluid, Pr (bar), feed, F (mm/rev), and depth of cut, D (mm).

Figure 13. The normal probability plot provides the closeness of the point to the median line; similarly, versus fits mentioned the distraction of the points away from the center. The histogram has the gapped vertical columns' shape with

frequencies. The versus order plot gives the reliability of the experiment results with more than half of the experiment counts. Then, Table 8 provides the SN ratio and mean-based outcomes in each trail of the four combinations.

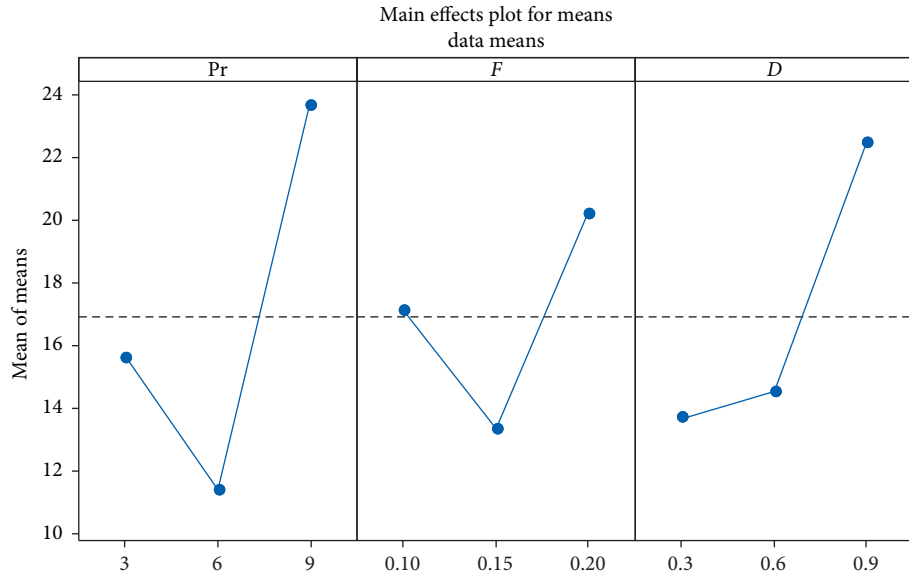


FIGURE 12: Tool wear, surface roughness, and thrust force focused on the important diagram based on the means; in the X-axis, Pr denotes pressure of cutting fluid (bar), F denotes feed (mm/rev), and D denotes depth of cut (mm).

TABLE 7: Tool wear, surface roughness, and thrust force-based response ratios of signal to noise.

Level	Pressure of cutting fluid, Pr (bar)	Feed, F (mm/rev)	Depth of cut, D (mm)
1	-26.41	-27.28	-26.17
2	-23.88	-25.39	-24.39
3	-31.22	-28.83	-30.95
Delta	7.34	3.44	6.56
Rank	1	3	2

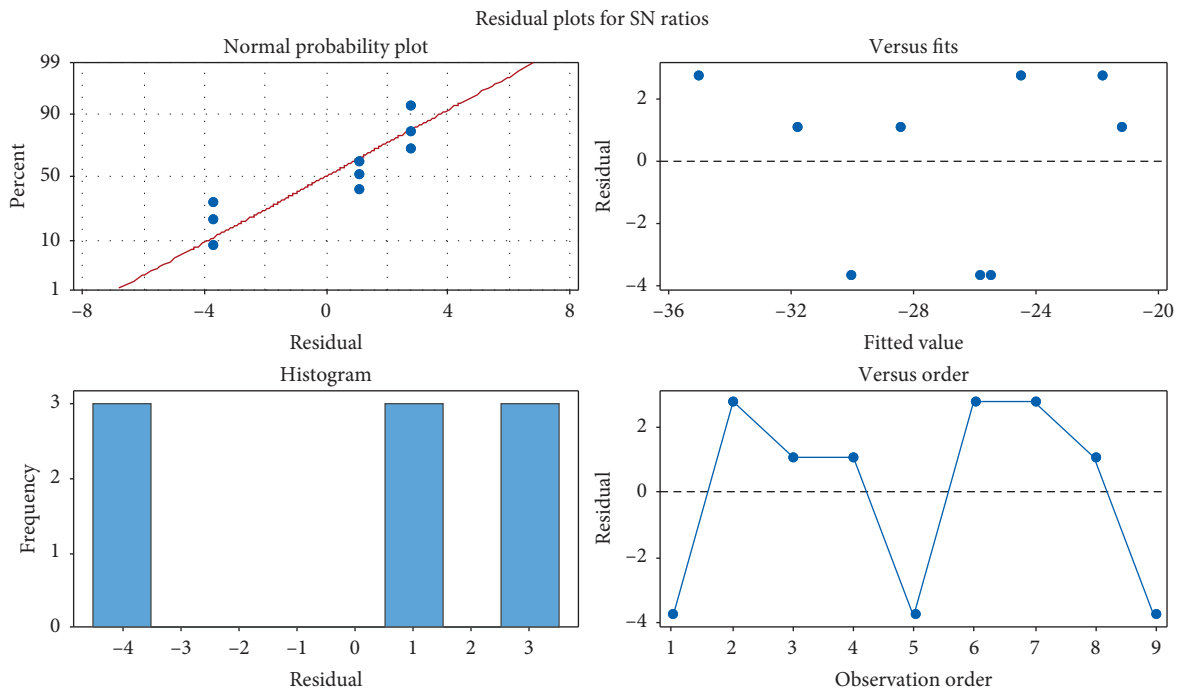


FIGURE 13: Tool wear, surface roughness, and thrust force-focused residual plot of percent, frequency, fitted values, and versus order.

TABLE 8: Cumulative outcome based on the signal-to-noise ratio and means in each trails' comparison.

No.	TW		SR		TF		TW, SR, and TF	
	SNRA 1	Mean 1	SNRA 2	Mean 2	SNRA 3	Mean 3	SNRA 4	Mean 4
1	-0.026	1.003	-11.799	3.890	-34.037	50.335	-29.294	18.409
2	6.143	0.493	-9.097	2.850	-23.742	15.385	-19.122	6.243
3	-3.767	1.543	-13.892	4.950	-35.563	59.998	-30.824	22.164
4	0.983	0.893	-7.121	2.270	-24.866	17.510	-20.178	6.891
5	-3.779	1.545	-11.150	3.610	-34.400	52.483	-29.653	19.213
6	3.702	0.653	-7.783	2.450	-26.506	21.150	-21.797	8.084
7	-3.197	1.445	-13.570	4.770	-37.124	71.814	-32.374	26.010
8	1.692	0.823	-7.568	2.390	-32.163	40.563	-27.408	14.592
9	-1.924	1.248	-13.368	4.660	-38.630	85.407	-33.872	30.438

4. Conclusion

This experimental study on optimization on operation parameters in the reinforced metal matrix of the AA6066 composite with HSS and Cu provided the following as the conclusions:

- (i) The machining can be possible for these conditions followed in the study
- (ii) Tool wear has cutting depth and feed as the most and least priority parameters, respectively
- (iii) Similarly, surface roughness has cutting depth and cutting fluid pressure as the greatest and smallest priority parameters correspondingly
- (iv) For the thrust force, cutting fluid pressure and cutting depth are the highest and lowest priority parameters
- (v) For all the response combinations, the pressure of the cutting fluid has the highest priority, and the feed has the least priority than the remaining input parameters
- (vi) The experimental results such as tool wear, surface roughness, and thrust force were reached at the parameters for the cutting fluid pressure of 6 bar with 0.15 mm per revolution of feed and 0.6 mm of cutting depth

Data Availability

The data used to support the findings of this study are included within the article and are also available from the corresponding author upon request.

Disclosure

This study was performed as a part of the Employment of Wolaita Sodo University, Wolaita Sodo, Ethiopia.

Conflicts of Interest

The authors declare that there are no conflicts of interest regarding the publication of this paper.

Acknowledgments

The authors thank Saveetha School of Engineering, Chennai, for the technical assistance to complete this experimental

work and appreciate the support from Wolaita Sodo University, Ethiopia.

References

- [1] T. Sathish and N. Sabarirajan, "Synthesis and optimization of AA 7175 - zirconium carbide (ZrC) composites machining parameters," *Journal of New Materials for Electrochemical Systems*, vol. 24, no. 1, pp. 34–37, 2021.
- [2] N. Sabarirajan, T. Sathish, and S. Karthick, "Machining parameters optimization of aluminium alloy 6063 with reinforcement of sic composites," *Materials Today: Proceeding*, vol. 33, no. 7, pp. 2559–2563, 2020.
- [3] P. Sevvell, T. Sathish, P. Sudharshan, and V. Vijayan, "Investigation and optimization of laser welding process parameters for AA7068 aluminium alloy butt joint," *Materials Today: Proceeding*, vol. 37, no. 2, pp. 1672–1677, 2021.
- [4] T. Sathish, "Experimental investigation of machined hole and optimization of machining parameters using electrochemical machining," *Journal of Materials Research and Technology*, vol. 8, no. 5, pp. 4354–4363, 2019.
- [5] S. Dinesh Kumar, T. Sathish, K. Muthukumar, and S. Karthick, "Natural inspiration technique for the parameter optimization of A-GTAW welding of naval steel," *Materials Today: Proceeding*, vol. 21, no. 1, pp. 843–846, 2020.
- [6] R. Saravanan, T. Sathish, K. Muthukumar, and V. Dhinakaran, "Study on temperature difference of aluminium nitride nanofluid used in solar flat plate collector over normal water," *AIP Conference Proceedings*, vol. 2283, no. 1, Article ID 020126, 2020.
- [7] K. Muthukumar, T. Sathish, S. Dinesh Kumar, and S. Karthick, "Temperature distribution analysis on diffusion bonded joints of Ti-6Al-4V with AISI 4140 medium carbon steel," *Materials Today: Proceeding*, vol. 21, no. 1, pp. 847–856, 2020.
- [8] S. P. Palaniappan, K. Muthukumar, R. V. Sabariraj, S. Dinesh Kumar, and T. Sathish, "CNC Turning process parameters optimization on Aluminium 6082 alloy by using Taguchi and ANOVA," *Materials Today: Proceeding*, vol. 21, no. 1, pp. 1013–1021, 2020.
- [9] S. Rajesh, D. Chandramohan, and T. Sathish, "Machining parameters optimization of surface roughness analysis for AA5083-Boron Carbide (B₄C) composites," *Materials Today: Proceeding*, vol. 33, no. 7, pp. 4642–4645, 2020.
- [10] K. Gurusami and T. Shalini Sand Sathish, "Optimization of stir casting parameters for corrosion rate analysis of AA7068-Boron carbide composites," *Materials Today: Proceeding*, vol. 33, no. 7, pp. 4650–4655, 2020.

- [11] R. Shetty, R. B. Pai, and S. S. Rao, "Rajesh nayak, "taguchi's technique in machining of metal matrix composites"" *Journal of the Brazilian Society of Mechanical Sciences and Engineering*, vol. 31, no. 1, pp. 12–20, 2009.
- [12] L. Natrayan, M. S. Santhosh, R. Mohanraj, and R. Hariharan, "Mechanical and tribological behaviour of Al_2O_3 & SiC reinforced aluminium composites fabricated via powder metallurgy," *IOP Conference Series: Materials Science and Engineering*, vol. 561, no. 1, Article ID 012038, 2019.
- [13] E. Georgantzia, M. Gkantou, and S. George, "Aluminium alloys as structural material: a review of research," *Engineering Structures*, vol. 227, Article ID 111372, 2021.
- [14] J. P. Davim, "Design optimization of cutting parameters for turning metal matrix composites based on the orthogonal arrays," *Journal of Materials Processing Technology*, vol. 132, pp. 340–344, 2003.
- [15] B. Vijaya Ramnath, C. Elanchezhian, RM. Annamalai, S. Aravind, V. Vignesh, and C. Subramanian, "Aluminium metal matrix composites - a review," *Reviews on Advanced Materials Science*, vol. 38, pp. 55–60, 2014.
- [16] M. Shukla, S. K. Dhakad, P. Agarwal, and M. K. Pradhan, "Characteristic behaviour of aluminium metal matrix composites: a review," *Materials Today: Proceeding*, vol. 5, pp. 5830–5836, 2018.
- [17] R. K. verma, L. Agrawal, and D. S. Awana, "Effect of variation of silicon and copper contents in aluminium-silicon copper Alloy," *International Journal of Engineering & Technology*, vol. 4, no. 1, pp. 149–156, 2013.
- [18] M. Singla, D. Dwivedi, L. Singh, and V. Chawla, "Development of aluminium based silicon carbide particulate metal matrix composite," *Journal of Minerals and Materials Characterization and Engineering*, vol. 8, no. 6, pp. 45–467, 2009.
- [19] K. K. Alaneme and A. O. Aluko, "Production and age-hardening behaviour of borax pre-mixed SiC Reinforced Al-Mg-Si alloy composites developed by double stir casting technique," *West Indian Journal of Engineering*, vol. 34, no. 1-2, pp. 80–85, 2012.
- [20] P. W. Pawar and A. Utpat, "Development of Aluminium based silicon carbide particulate metal matrix composites for spur Gear," *Procedia materials science*, vol. 6, pp. 1150–1156, 2014.
- [21] L. Natrayan, V. Sivaprakash, and M. S. Santhosh, "Mechanical, microstructure and wear behavior of the material AA6061 reinforced SiC with different leaf ashes using advanced stir casting method," *International Journal of Engineering and Advanced Technology*, vol. 8, pp. 366–371, 2018.
- [22] N. Anjibabu Merneedi, M. Rao, and V. V. Subbaroa, "Free vibration analysis of an elliptical plate with cut-out," *Journal of Vibro Engineering*, vol. 19, no. 4, pp. 2341–2353, 2017.
- [23] L. Natarayan and A. Merneedi, "Experimental investigation on wear behaviour of bio-waste reinforced fusion fiber composite laminate under various conditions," *Materials Today: Proceedings*, vol. 37, no. 2, pp. 1486–1490, 2021.
- [24] N. Anjibabu Merneedi, M. Rao, and V. V. Subbaroa, "Free vibration analysis of a thin rectangular plate with multiple circular and rectangular cut-outs," *Journal of Mechanical Science and Technology*, vol. 31, no. 11, pp. 5185–5202, 2017.